# A Random Matrix Model for Color Superconductivity at Zero Chemical Potential

Benoît Vanderheyden and A. D. Jackson

The Niels Bohr Institute, Blegdamsvej 17, DK-2100 Copenhagen Ø, Denmark.

(August 12, 2009)

## Abstract

We discuss random matrix models for the spontaneous breaking of both chiral and color symmetries at zero chemical potential and finite temperature. Exploring different Lorentz and gauge symmetric color structures of the random matrix interactions, we find that spontaneous chiral symmetry breaking is always thermodynamically preferred over diquark condensation. Stable diquark condensates appear only as $SU(2)$ rotated chiral condensates, which do not represent an independent thermodynamic phase. Our analysis is based on general symmetry arguments and hence suggests that no stable and independent diquark phase can form in QCD with two flavors at zero quark chemical potential.

# I. INTRODUCTION

The exploration of the phase diagram of QCD is of fundamental interest for understanding the nature of strongly interacting matter at high temperatures and densities and its implications for the physics of heavy-ion collisions and neutron stars. One central aim of studies of the phase diagram is to determine how its global structure is shaped by underlying symmetries, their spontaneous breaking, and their interplay.

The current picture of the QCD phase transitions is shaped by various symmetry breaking patterns [1,2]. For QCD with two light flavors, lattice simulations [3] indicate the restoration of chiral symmetry for temperatures above $T \sim 160$ MeV as one moves along the zero baryon density axis. This phase transition is of second order. Along the zero temperature axis, one expects chiral restoration to proceed at high densities through a first-order transition [1]. Because QCD is asymptotically free, it is also likely that a transition to a plasma of deconfined quarks and gluons occurs at the same high densities required for the screening of color interactions. The ground state of this weakly coupled plasma may be dominated by quark-quark correlations as suggested by early and recent works [4,5,7,8]: the attractive quark-quark interaction may lead to the formation of quark Cooper pairs, which spontaneously break color gauge symmetry. Nambu-Jona-Lasinio models [5,6] and instanton-based calculations [7,8] suggest sizeable diquark condensates with $\langle qq \rangle \sim 100$ MeV at quark chemical potentials $\mu \sim 300$ MeV or higher.

Current microscopic models of color superconductivity [4–8] are all implemented at mean-field level and, although different in their treatment of the primary interaction among quarks, have the following schematic phase diagram. Diquark condensates appear at the low densities usually associated with broken chiral symmetry, but they are unstable. They are found to be stable in the high density, chiral symmetric phase. Between these two limits, a state where both chiral and color symmetries are broken appears either as a saddle point of the thermodynamical potential [7], or as a global minimum [8]. Given the range of treatments of the QCD interactions, it is desirable to understand the extent to which predictions of

diquark condensation are model-independent. This leads to the question of determining how the phase diagram is shaped by global symmetries on one hand and by the detailed dynamics of the interactions on the other.

We wish to address this question by means of random matrix methods applied to $SU(3)$ QCD with two flavors. As in lattice calculations, significant complications arise from the non-Hermitean character of the Dirac operator in models with a finite quark chemical potential. Because our main goal is to set the stage for studying diquark condensation, we shall confine our present exploration to Hermitean matrix models with zero chemical potential.

Before introducing our method in detail, let us briefly recall the principles and motivations of existing random matrix models for chiral symmetry breaking [9] since our formulation will follow in a similar spirit. Chiral random matrix models ($\chi$RMM) study the spectrum of the Euclidean Dirac operator in a theory that respects all global symmetries of QCD, but in which the detailed dynamics of the interaction among quarks is replaced by averages over random matrices. The chiral order parameter, $< \bar{\psi}\psi >$, can be obtained from the density of the smallest eigenvalues of the Dirac operator with the aid of the Banks-Casher formula [10], and properties of the phase diagram can thus be determined. The primary advantage of such an approach lies in its universality [11]. The statistical properties of the small eigenvalues, and thus mean-field predictions regarding the chiral phase transition, depend only on the symmetries of the Dirac operator. They do not depend on the particular procedure used to average over the random interactions. In particular, chiral random matrix models reproduce the mean-field exponents expected for QCD with two light flavors [12].

In this paper, we consider a random matrix model in which both chiral and diquark condensation can take place and study the competition between these two forms of order. The paper is organized as follows. In Section II, we start by constructing a class of interactions that include chiral and color symmetries. The dynamics of the interactions are described by Gaussian averages over random matrices. In Section III, we study the four-fermion potentials produced by integration over all possible choices of Lorentz invariant and

3

gauge symmetric interactions. Particular combinations of these choices give rise to four-fermion interactions of the form encountered in instanton and NJL models. In Section IV, we introduce auxiliary variables in the usual way, derive the thermodynamical potential, and determine the resulting phase diagram in parameter space. As we discuss in Section V, strong dynamical constraints on the coupling parameters prevent the exploration of certain regions of the phase diagram. It results that the spontaneous breaking of chiral symmetry is thermodynamically preferable to diquark condensation in all cases. Stable diquark condensates can appear at most as $SU(2)$ rotated chiral condensates, which belong to a broken chiral symmetry phase. This case is considered in detail in section VII. Our analysis of the phase diagram clearly distinguishes between features that directly follow from global symmetries and those that are model-dependent. We illustrate this point in Section VI, where we compare our phase diagram to the predictions of NJL model studies.

Not all the interactions to be considered here are directly related to QCD. However, our arguments are based on simple symmetry considerations that also apply to QCD. This suggests that no mean-field treatment of QCD with two light flavors can find stable diquark condensates at zero chemical potential.

## II. CONSTRUCTION OF A RANDOM MATRIX MODEL

We now turn to the construction of a random matrix model suitable for the exploration of diquark condensation as well as chiral symmetry breaking. Since the order parameter for color superconductivity is overall antisymmetric in flavor, spin, and color, these quantum numbers should explicitly be included in the model. The extended block structure of the resulting random matrix model is somewhat complicated. This is an unavoidable consequence of our desire to permit the competition between two distinct mechanisms for spontaneous symmetry breaking. Fortunately, the description of the QCD partition function that will emerge from our analysis is very simple. While we will discuss in later sections how our results naturally follow from global symmetries, we now focus on the detailed description of

4

the model.

A natural starting point is to extend the $\chi$RMM [9] by decomposing each chiral subblock of the single quark propagator into matrices with a flavor, spin, and color, block structure. This results in a vector theory which, as we show later, does not support diquark condensation at zero quark chemical potential. We wish to explore further possibilities of matrix models that build correlations in the diquark channel, and study the resulting symmetry breaking patterns. We are forced in the process to give up some of the symmetries of QCD. However, as we discuss later in length, our exploration brings insight into the question of how global symmetries shape the phase diagram.

In the following, we only consider models for which the single quark propagator is Hermitean. This choice ensures that the chiral and diquark order parameters can unambiguously be related to the spectral properties of the Dirac operator. We further impose the Dirac operator to have a $4 \times 4$ Lorentz invariant block structure in the vacuum, and a color symmetric $N_c \times N_c$ block structure. Once the flavor, spin, and color structure have been specified, one is left with $N \times N$ block matrices. It should be stressed that the physical meaning of the matrix size $N$ here is different from that in $\chi$RMM. Because we explicitly include color degrees of freedom, we can no longer make analogies with instanton overlap matrices, nor can we directly relate $N$ to the density of zero modes. Ultimately, we will discuss various interactions by comparing the four-point potentials induced by the random background in the chiral and diquark channels. Hence, we regard the thermodynamic limit $N \to \infty$ as a way to obtain mean-field results from these potentials. The connection to zero modes is not lost, however, as one still expects that order parameters depend only on the dynamics of the smallest eigenvalues of the Dirac operator.

Assuming a zero vacuum angle, the finite temperature partition function has the form

$$
\begin{aligned}
Z(T) = \int \mathcal{D}H \, \mathcal{D}\psi_1^\dagger \, \mathcal{D}\psi_1 \, \mathcal{D}\psi_2^T \, \mathcal{D}\psi_2^* \\
\times \exp\left[ i \begin{pmatrix} \psi_1^\dagger \\ \psi_2^T \end{pmatrix} \begin{pmatrix} \mathcal{H} + \mathcal{T} + im & \eta P_\Delta \\ -\eta^* P_\Delta^\dagger & -\mathcal{H}^T + \mathcal{T} - im \end{pmatrix} \begin{pmatrix} \psi_1 \\ \psi_2^* \end{pmatrix} \right],
\end{aligned}
\tag{1}
$$

where 1 and 2 denote flavors and where $\psi_1$, $\psi_1^\dagger$, $\psi_2^T$, and $\psi_2^*$ are independent Grassmann variables which are not related by complex conjugation or transposition. $\mathcal{H}$ is intended to mimic the interaction of a single quark with a gluon background, and $\mathcal{D}H$ is the random matrix measure, which we will write explicitly below. We have adopted a Nambu-Gorkov representation for the flavor structure by transposing the single quark operator for flavor 2. This representation enables the random matrix interactions to build correlations between states with the same baryon number. We also include external mass and diquark parameters $m$ and $\eta$. These parameters permit the selection of a particular direction for chiral and color symmetry breaking and are to be taken to zero in an appropriate order at the end of the calculations. The mass $m$ is a color diagonal matrix, associated with the chiral order parameters $\langle \psi_1^\dagger \psi_1 \rangle$ and $\langle \psi_2^T \psi_2^* \rangle$. The complex quantity $\eta$ is to be associated with the diquark order parameters $\langle \psi_2^T P_\Delta \psi_1 \rangle$ and $\langle \psi_1^\dagger P_\Delta \psi_2^* \rangle$. We consider here the pattern of chiral symmetry breaking expected in QCD [17]. We also consider diquark condensates in a $\bar{3}$ state, i.e., in a scalar state which is antisymmetric in spin and in the condensing colors. Hence, $P_\Delta \equiv C \gamma^5 (i\lambda_2)$, where $C$ is the charge conjugation matrix, and $i\lambda_2$ is antisymmetric in colors 1 and 2.

The temperature $T$ enters the model in the usual manner [12] through the chiral block matrix

$$\mathcal{T} = \begin{pmatrix} 0 & \pi T \\ \pi T & 0 \end{pmatrix}, \tag{2}$$

where only the lowest Matsubara frequency has been retained. In Eq. (1), $\mathcal{T}$ appears twice with a positive sign. This corresponds to taking opposite Matsubara frequencies for each flavor. This choice is justified for s-wave pairing which, in microscopic models, leads to a homogeneous order parameter, $< \psi_2^T(x) P_\Delta \psi_1(0) > \sim \Delta$, and thus mixes Fourier components with opposite four-momenta.

We write the Dirac operator $\mathcal{H}$ as an expansion into a direct product of the 16 Dirac matrices $\Gamma_C$, times $N_c^2$ color matrices:

$$\mathcal{H}_{\lambda i \alpha k; \kappa j \beta l} = \sum_{C=1}^{16} \left( \Gamma_C \right)_{\lambda i; \kappa j} \sum_{a=1}^{N_c^2} \Lambda_{\alpha\beta}^a \left( A_{\lambda\kappa}^{Ca} \right)_{kl}. \tag{3}$$

Here, the indices $(\lambda,\kappa)$, $(i,j)$, and $(\alpha,\beta)$ respectively denote chiral, spin, and color quantum numbers. The indices $(k,l)$ run from 1 to $N$. The terms $\Lambda^a$ represent the color matrices $\lambda^a$ when $a \leq N_c^2 - 1$ and the diagonal matrix $(\delta_c)_{\alpha\beta} = \delta_{\alpha\beta}$ when $a = N_c^2$. The normalization for color matrices is $\mathrm{Tr}[\lambda^a\lambda^b] = 2\delta_{ab}$ and $\mathrm{Tr}[\delta_c^2] = N_c$; the normalization of the Dirac matrices is $\mathrm{Tr}[\Gamma_C\Gamma_{C'}] = 4\delta_{CC'}$. In the remainder of the paper we will explicitly keep track of $N_c$ factors, but we will eventually be interested in the case $N_c = 3$.

The random matrices $A_{\lambda\kappa}^{Ca}$ represent the fields mediating the interaction between quarks and are thus real. Their detailed character depends on the chiral structure of $\Gamma_C$. In a chiral basis, the Dirac operator for vector or axial interactions has the form

$$\mathcal{H}_{\mathrm{V,A}} = \begin{pmatrix} 0 & W \\ W^\dagger & 0 \end{pmatrix}, \tag{4}$$

where, according to Eq. (3), $W = (\Gamma_{\mathrm{V,A}})_{\mathrm{RL}} \sum_a \Lambda^a A_{\mathrm{RL}}^{Ca}$ and $W^\dagger = (\Gamma_{\mathrm{V,A}})_{\mathrm{LR}} \sum_a \Lambda^a A_{\mathrm{LR}}^{Ca}$. Since $\mathcal{H}$ is Hermitean, we have $A_{\mathrm{LR}}^{Ca} = (A_{\mathrm{RL}}^{Ca})^T$. In the cases of scalar, pseudoscalar, and tensor interactions, the Dirac operator takes the form

$$\mathcal{H}_{\mathrm{S,P,T}} = \begin{pmatrix} X & 0 \\ 0 & Y \end{pmatrix}, \tag{5}$$

where $X = (\Gamma_{S,P,T})_{\mathrm{RR}} \sum_a \Lambda^a A^{Ca}$ and $Y = (\Gamma_{S,P,T})_{\mathrm{LL}} \sum_a \Lambda^a A^{Ca}$ are Hermitean. For the scalar and pseudoscalar cases and for some of the six tensor matrices, $X$ and $Y$ are spin-diagonal and thus must be described by real symmetric matrices $A^{Ca}$. As a consequence of rotational invariance, the matrices $A^{Ta}$ associated with spin off-diagonal components of the tensor interaction must also be real symmetric.

The vector interactions mimic single-gluon exchange and respect the global symmetries of QCD. All other interactions break at least one of them. Axial interactions are absent in QCD and, in a four-dimensional field theory, may spontaneously break parity. Scalar, pseudoscalar, and tensor interactions, break axial symmetry explicitly and may break isovector

symmetry spontaneously through the formation of $\langle \psi_R^\dagger \psi_L \rangle$ and $\langle \psi_L^\dagger \psi_R \rangle$ condensates. This latter condensation can actually be avoided by retaining a finite mass parameter $m$ until the end of the calculation so that it is always thermodynamically preferable to break symmetry in the axial rather than vector channel. We could extend our exploration to interactions containing the generators $\tau_i$ of $SU(2)$ flavor and study the ensuing effective four-fermion potentials. Here, however, we will not adopt such an approach. It will be seen from the discussion below that the addition of further flavor symmetry will not change our conclusions.

Having specified the random matrices $A_{\lambda\kappa}^{Ca}$, we now define the measure $\mathcal{D}H$

$$\mathcal{D}H = \left\{ \prod_{Ca} \prod_{\lambda\kappa} \mathcal{D}A_{\lambda\kappa}^{Ca} \right\} \exp\left[ -N \sum_{Ca} \sum_{\lambda\kappa} \beta_C \Sigma_{Ca}^2 \, \mathrm{Tr}[A_{\lambda\kappa}^{Ca}(A_{\lambda\kappa}^{Ca})^T] \right], \qquad (6)$$

where $\mathcal{D}A_{\lambda\kappa}^{Ca}$ are Haar measures. The index $\beta_C$ is $\beta_C = 1$ for real matrices ($C = V, A$) and $\beta_C = 1/2$ for real symmetric matrices ($C = S, P, T$). In order to respect color symmetry, the members of each $N_c^2 - 1$ color multiplet share the same variance. In other words, $\Sigma_{Ca} = \Sigma_{C|O}$ for $1 \leq a \leq N_c^2 - 1$, and $\Sigma_{Ca} = \Sigma_{C|S}$ for the singlet component ($a = N_c^2$). Further, once the color channel $a = S, O$ has been chosen, we respect Lorentz invariance in the vacuum by requiring a common variance $\Sigma_{T|S,O}$ for each of the six components of the tensor interaction. The four components of the vector and axial interactions are characterized by the variances $\Sigma_{V|S,O}$ and $\Sigma_{A|S,O}$.

<div align="center">

### III. TOWARDS A NON-LINEAR SIGMA MODEL

</div>

We can solve the model of Eq. (1) exactly by standard methods. The first step is to perform the Gaussian integration over the matrix elements. This leads to a four-fermion interaction $\mathcal{Y}$ and a partition function of the form

$$Z(T) = \int \mathcal{D}\psi_1^\dagger \mathcal{D}\psi_1 \mathcal{D}\psi_2^T \mathcal{D}\psi_2^* \, \exp\left[ \mathcal{Y} + i \begin{pmatrix} \psi_1^\dagger \\ \psi_2^T \end{pmatrix} \begin{pmatrix} \mathcal{T} + im & \eta P_\Delta \\ -\eta^* P_\Delta^\dagger & \mathcal{T} - im \end{pmatrix} \begin{pmatrix} \psi_1 \\ \psi_2^* \end{pmatrix} \right]. \qquad (7)$$

By introducing auxiliary variables, one can then derive a non-linear sigma model, the saddle point of which provides the exact solution to the original model in the limit $N \to \infty$. In

this section, we concentrate on the fate of the diquark and the chiral condensates and thus consider only the relevant auxiliary variables. While it is largely a technical matter, it is important to note that the four-point interaction has a slightly different structure depending on whether the interaction is either vector or axial or is either scalar, pseudoscalar, or tensor. We now discuss these two cases separately.

### A. Vector and axial interactions $(C = V, A)$

Integrating out the real matrices $A_{\mathrm{RL}}^{Ca}$ produces a four-point interaction of the form[1]

$$\mathcal{Y}_C = -\sum_{\mu a} \frac{1}{8N\Sigma_{Ca}^2} \sum_{k,l=1}^{N} (J_{kl}^{\mu a})^2, \tag{8}$$

where the quark current $J^{\mu a}$ is

$$J_{kl}^{\mu a} = \psi_{1Rk}^{\dagger} \, \Gamma_{RL}^{\mu} \Lambda^a \, \psi_{1Ll} + \psi_{1Ll}^{\dagger} \, \Gamma_{LR}^{\mu} \Lambda^a \, \psi_{1Rk}$$
$$- \psi_{2Rk}^{T} (\Gamma_{LR}^{\mu})^T (\Lambda^a)^T \, \psi_{2Ll}^{*} - \psi_{2Ll}^{T} (\Gamma_{RL}^{\mu})^T (\Lambda^a)^T \, \psi_{2Rk}^{*}, \tag{9}$$

and where $\Gamma^{\mu} = \gamma^{\mu}$ and $\Gamma^{\mu} = i\gamma^{\mu}\gamma^5$ for vector and axial interactions, respectively. When taking the square of $J_{kl}^{\mu a}$ in Eq. (8), we need retain only those cross-terms relevant to chiral and diquark condensates. This becomes clear after suitable Fierz transforms of the Lorentz and color operators. Consider, for example, the four-point interaction resulting from the $N_c^2 - 1$ color multiplet, $\Lambda^a = \lambda^a$. Denoting the Fierz coefficient in the chiral channel by $f_\chi^O$, the cross-term between the first and second terms in Eq. (9) gives

$$\sum_{\mu=1}^{4} \sum_{a=1}^{N_c^2-1} (\Gamma_{RL}^{\mu})_{ij} \, \lambda_{\alpha\beta}^a \times (\Gamma_{LR}^{\mu})_{i'j'} \, \lambda_{\alpha'\beta'}^a = f_\chi^O \, \delta_{ij'}\delta_{\alpha\beta'} \times \delta_{i'j}\delta_{\alpha'\beta} + \cdots, \tag{10}$$

and leads to a four-point interaction of the form

$$\mathcal{Y} \sim + \frac{f_\chi^O}{4N\Sigma_{C|O}^2} \, \sum_{k} \psi_{1Rk}^{\dagger}\psi_{1Rk} \times \sum_{l} \psi_{1Ll}^{\dagger}\psi_{1Ll} \, , \tag{11}$$

---

[1]Note that the product $\mathrm{Tr}[A_{RL}^{Ca} A_{LR}^{Ca}]$ appears twice in the measure; hence the factor 8.

which is relevant for the formation of a chiral condensate $< \psi^\dagger \psi >$. Similarly, the cross-term between the first and fourth terms in Eq. (8) can be projected onto a product of diquark bilinears by means of the transformation

$$-\sum_{\mu=1}^{4} \sum_{a=1}^{N_c^2-1} (\Gamma_{RL}^\mu)_{ij} \lambda_{\alpha\beta}^a \times (\Gamma_{RL}^\mu)_{i'j'}^T (\lambda^a)_{\alpha'\beta'}^T = f_\Delta^O \, \varepsilon_{ij'} \, (i\lambda_2)_{\alpha\beta'} \times \varepsilon_{i'j} \, (i\lambda_2)_{\alpha'\beta} + \cdots, \qquad (12)$$

where $f_\Delta^O$ is now the Fierz coefficient in the diquark channel, while $\varepsilon = (C\gamma^5)_{\mathrm{RR}} = (C\gamma^5)_{\mathrm{LL}}$ and $(i\lambda_2)_{\alpha\beta}$ are respectively spin and color antisymmetric tensors. This transformation leads to the four-fermion interaction

$$\mathcal{Y} \sim + \frac{f_\Delta^O}{4N\Sigma_{C|O}^2} \, \sum_k \psi_{1Rk}^\dagger \, (i\,\varepsilon\,\lambda_2) \, \psi_{2Rk}^* \times \sum_l \psi_{2Ll}^T \, (i\,\varepsilon\,\lambda_2) \, \psi_{1Ll}, \qquad (13)$$

which is relevant for the formation of a diquark condensate $< \psi_2^T P_\Delta \psi_1 >$.

Transposing the Dirac operators in Eqs. (10) and (12) provides us with the relations needed to transform the cross-terms between the third and fourth terms and between the second and third terms in Eq. (9). Taking into account the contributions from the $N_c^2 - 1$ color multiplet and the color singlet leads then to the total four-point interaction

$$\mathcal{Y}_C = +\frac{1}{4N} \sum_{a=O,S} \frac{1}{\Sigma_{C|a}^2} \sum_{k,l} \Big\{ f_\chi^a \Big( \psi_{1Rk}^\dagger \psi_{1Rk} \times \psi_{1Ll}^\dagger \psi_{1Ll} + \psi_{2Rk}^T \psi_{2Rk}^* \times \psi_{2Ll}^T \psi_{2Ll}^* \Big)$$
$$+ f_\Delta^a \Big( \psi_{1Rk}^\dagger \, (i\varepsilon\lambda_2) \, \psi_{2Rk}^* \times \psi_{2Ll}^T \, (i\varepsilon\lambda_2) \, \psi_{1Ll} + \psi_{1Ll}^\dagger \, (i\varepsilon\lambda_2) \, \psi_{2Ll}^* \times \psi_{2Rk}^T \, (i\varepsilon\lambda_2) \, \psi_{1Rk} \Big) \Big\}. \quad (14)$$

### B. Scalar, pseudoscalar, and tensor interactions ($C = S, P, T$)

The random matrices representing the interaction in the scalar, pseudoscalar and tensor channels are real symmetric. Their integration produces the four-fermion interaction

$$\mathcal{Y}_{\mathrm{C}} = -\sum_{a\mu} \frac{1}{16N\Sigma_{C|a}^2} \sum_{kl} (J_{kl}^{a\mu} + J_{lk}^{a\mu})^2, \qquad (15)$$

where $a$ again denotes the color channel ($a = O, S$) and, in the case of a tensor interaction, $\mu = 1, \ldots, 6$ labels the six antisymmetric Dirac matrices. The quark current here is

$$J_{kl}^{a\mu} = \psi_{1Rk}^\dagger \, (\Gamma_C^\mu)_{\mathrm{RR}} \Lambda^a \, \psi_{1Rl} - \psi_{2Rl}^T \, (\Gamma_C^\mu)_{\mathrm{RR}}^T (\Lambda^a)^T \, \psi_{2Rk}^* + \{\mathrm{R} \leftrightarrow \mathrm{L}\}. \qquad (16)$$

10

Once again, only some of the cross-terms in Eq. (15) contribute to the chiral and diquark channels. After the necessary Fierz transforms, these terms lead to the four-fermion interaction

$$\mathcal{Y}_{\mathrm{C}} = \sum_a \frac{1}{8N\Sigma_{C|a}^2} \sum_{k,l} \left\{ f_\chi^a \left( (\psi_{1Rk}^\dagger \psi_{1Rk})^2 + (\psi_{2Rk}^T \psi_{2Rk}^*)^2 \right) \right.$$
$$\left. + 2 f_\Delta^a\, \psi_{1Rk}^\dagger\, (i\varepsilon\lambda_2)\, \psi_{2Rk}^* \times \psi_{2Rl}^T\, (i\varepsilon\lambda_2)\, \psi_{1Rl} + \{\mathrm{R} \leftrightarrow \mathrm{L}\} \right\}. \tag{17}$$

## IV. PHASE DIAGRAM IN PARAMETER SPACE

We are now in a position to derive a non-linear sigma model from the total four-point interaction, $\mathcal{Y} = \sum_C \mathcal{Y}_C$ with $\mathcal{Y}_C$ given by Eqs. (14) and (17). We first write $\mathcal{Y}$ as the sum of squares of fermion bilinears and then transform the quartic terms into fermion bilinears by means of the Hubbard-Stratonovich formula

$$\exp(-AQ^2) \sim \int d\sigma \exp(-\frac{\sigma^2}{4A} + iQ\sigma), \tag{18}$$

which introduces an auxiliary field $\sigma$. A number of simplifications now follow if one is interested only in those correlations among quark states which contribute to chiral and diquark condensates. We anticipate that the saddle points of our non-linear sigma model will be described in the space of auxiliary variables by dynamical masses that are real and independent of chirality and flavor and by complex pairing potentials that are independent of chirality. In the following, we restrict our attention to such choices and introduce accordingly real chiral and complex diquark fields $\sigma$ and $\Delta$.

Before proceeding, we also consider the possibility that a spontaneous breaking of the color symmetry affects the chiral order parameters. This possibility clearly arises in the instanton model of color superconductivity of Carter and Diakonov [7]. These authors pointed out that the masses of the quarks with the condensing colors must be different from those with the transverse colors if the Dyson-Gorkov equations are to close. To take this effect into account in the present formulation, we include the projections of the original interaction

onto a chiral channel with color quantum numbers described by the diagonal generator $\lambda_8$. This introduces an additional Fierz constant $f_8^a$, a term $f_8^a \, \delta_{ij'}(\lambda_8)_{\alpha\beta'} \times \delta_{i'j}(\lambda_8)_{\alpha'\beta}$ on the right side of Eq. (10), and a chiral field $\sigma_8$. With these additions, the chiral fields couple to quarks in the color diagonal combination $\psi^\dagger(\sigma + \sigma_8\lambda_8)\psi$. This can also be written as $\psi^\dagger\sigma_c\psi$ where $\sigma_c \equiv \mathrm{diag}(\sigma_1, \sigma_1, \sigma_3)$ with

$$\sigma_1 \equiv \sigma + \frac{\sigma_8}{\sqrt{3}} \quad \text{and} \quad \sigma_3 \equiv \sigma - 2\frac{\sigma_8}{\sqrt{3}}. \tag{19}$$

This final form of the fermion bilinear makes the separation in the chiral fields explicit. We follow this pattern in the external masses by taking $m = \mathrm{diag}(m_1, m_1, m_3)$.

The derivation of the sigma model potential is now straightforward. Keeping only the three auxiliary variables $\sigma_1$, $\sigma_3$, and $\Delta$, the total four-fermion interaction $\mathcal{Y}$ becomes

$$\exp\mathcal{Y} \sim \int d\sigma_1 d\sigma_3 d\Delta \, \exp\left[-4N\left(A|\Delta|^2 + B(2\sigma_1 + \sigma_3)^2/9 + C(\sigma_1 - \sigma_3)^2/3\right)\right.$$
$$\left. + \begin{pmatrix} \psi_{1R}^\dagger \\ \psi_{2R}^T \end{pmatrix} \begin{pmatrix} -\sigma_c & -\Delta\varepsilon\lambda_2 \\ \Delta^*\varepsilon\lambda_2 & \sigma_c \end{pmatrix} \begin{pmatrix} \psi_{1R} \\ \psi_{2R}^* \end{pmatrix} + \{\mathrm{R} \leftrightarrow \mathrm{L}\}\right], \tag{20}$$

where we have explicitly factored out chiral and spin factors in the terms quadratic in auxiliary variables. The coupling constants $A$, $B$, and $C$ are given as

$$A \equiv 2\left(\sum_{Ca} \frac{f_\Delta^a}{\Sigma_{Ca}^2}\right)^{-1} \quad B \equiv 2\left(\sum_{Ca} \frac{f_\chi^a}{\Sigma_{Ca}^2}\right)^{-1} \quad C \equiv 2\left(\sum_{Ca} \frac{f_8^a}{\Sigma_{Ca}^2}\right)^{-1}. \tag{21}$$

Inserting then Eq. (20) in Eq. (7), we obtain the partition function of Eq. (1). Integrating out the fermion fields, we have

$$Z(T) \sim \int d\sigma_1 \, d\sigma_3 \, d\Delta \, \exp\left[-4N\Omega(\sigma_1, \sigma_3, \Delta)\right], \tag{22}$$

where the thermodynamic potential $\Omega$ is

$$\Omega(\sigma_1, \sigma_3, \Delta) = A|\Delta|^2 + B\left(\beta_1\sigma_1^2 + \beta_2\sigma_1\sigma_3 + \beta_3\sigma_3^2\right) - (N_c - 2)\log[(\sigma_3 + m_3)^2 + \pi^2 T^2]$$
$$- 2\log[(\sigma_1 + m_1)^2 + |\Delta + \eta|^2 + \pi^2 T^2], \tag{23}$$

and where

$$\beta_1 \equiv \frac{4}{9} + \frac{1}{3}C/B, \quad \beta_2 \equiv \frac{4}{9} - \frac{2}{3}C/B, \quad \beta_3 \equiv \frac{1}{9} + \frac{1}{3}C/B. \tag{24}$$

Again, the external masses $m_1$ and $m_3$ and the parameter $\eta$ are to be taken to zero at the end of the calculation.

The thermodynamic stable phases are given by the minima of the potential $\Omega$ in Eq. (23). In practice, one does not expect any condensation in repulsive channels; the global minimum must give zero for the corresponding variables. In the following we therefore consider the $\Omega$ as given in Eq. (23) only in cases where the chiral-$\lambda_8$ channel is attractive and $C$ is positive. In cases where the chiral channel $\lambda_8$ is repulsive, or $C < 0$, we will explicitly set $\sigma_1 = \sigma_3$ as the field $\sigma_8 = (\sigma_1 - \sigma_3)/\sqrt{3}$ is assumed not to condense.

In spite of the complications present in the initial formulation of this model and its interactions, the potential $\Omega$ of Eq. (23) has a very simple structure. In particular, we note that it depends only on three coupling parameters, $A$, $B$, and $C$. The arguments in the logarithms of Eq. (23) represent squares of typical excitation energies in the system. Because of color mixing in the diquark channel, these excitations lead in the case of two colors to a gap $\Delta$ in addition to the dynamical mass $\sigma_1$. The remaining colors develop a mass $\sigma_3$, which is in general coupled to $\sigma_1$. The question of whether chiral or color symmetry breaking is preferred is now determined by the relative strengths of the $\sigma$ and $\Delta$ fields. This strength ratio depends solely on the ratio $B/A$ or, equivalently, on the ratio of the Fierz projections of the original interaction onto diquark and chiral channels, $B/A \sim f_\Delta^a / f_\chi^a$. The ratio $C/B$ plays a secondary role, as it determines the symmetry breaking pattern only when all three auxiliary fields acquire non-zero mean field values.

In the large $N$ limit, the thermodynamically stable phases are determined by the saddle points of the potential $\Omega$, Eq. (23). We find that $\Omega$ has precisely one local minimum for each fixed value of the coupling parameters and the temperature. There are thus only second order transitions between single phases. The variation of $B/A$, $C/B$, and $T$ reveals a rich phase structure which is illustrated in Fig. 1. Choosing the ratio $B/A$ fixes the slope of a straight line in parameter space passing through the origin. Increasing the temperature $T$

corresponds to moving along that line from the origin to large values of the axis coordinates.

It is useful at this stage to repeat our objective. The only interaction that represents QCD is single-gluon exchange, which is a color octet, flavor diagonal, and Lorentz vector interaction. This interaction realizes a ratio $B/A = 3/4$ for $N_c = 3$. This corresponds to the dot-dashed line in Fig. 1. All other interactions break at least one of the symmetries of QCD. However, a study of these deformations of QCD is useful on two respects. First, as discussed shortly, it reveals that the phase diagram is mostly shaped by color rather than chiral symmetry. Second, as discussed in Section VI, a comparison to the phase diagram of microscopic models shows what aspects of the phase transition are protected by symmetry. We now turn to a description of the phase diagram assuming that the parameters $A$, $B$, and $C$, are chosen freely. We will later consider what ranges of values these parameters can actually take, given that they follow from a single primary interaction, Eq. (21).

We find the usual chiral phase transition whenever $B/A < N_c/2$. In particular, $\Delta = 0$ and $\sigma_1 = \sigma_3$. The potential $\Omega$ then has the saddle-point solutions found in the $\chi$RMM at finite temperature [12], and thus reproduces mean-field critical exponents. The system breaks chiral symmetry spontaneously at low temperatures $T < T_\chi$ with $T_\chi^2 = N_c/(\pi^2 B)$. Below $T_\chi$, we find chiral fields with a square root dependence in the temperature, $\sigma_1 = \sqrt{N_c/B}\sqrt{1 - T^2/T_\chi^2}$ [12]. Above $T_\chi$, chiral symmetry is restored and $\sigma_1 = \sigma_3 = 0$. Spontaneous breaking of color symmetry occurs only for ratios $B/A$ larger than $N_c/2$. This region of parameter space contains three phases. First, large values of $B$ favor chiral symmetric phases, $\sigma_1 = \sigma_3 = 0$. In this case, color is spontaneoulsy broken below the critical temperature $T_\Delta = 2/(\pi^2 A^2)$, and is restored above. We again find a square root dependence for the pairing gap below $T_\Delta$, $\Delta = \sqrt{2/A}\sqrt{1 - T^2/T_\Delta^2}$. Second, keeping $A$ fixed to values $A < 2/(\pi^2 T^2)$ and decreasing $B$ from large values, one encounters a phase of mixed symmetry breaking where all condensates are developed and where $\sigma_1 \neq \sigma_3$. The upper boundary of this phase depends on $C$; we have plotted three examples of this critical line in Fig. 1.

Before further discussing the nature of the mixed symmetry breaking phase, we must

14

distinguish cases where the chiral-$\lambda_8$ channel is attractive and $C > 0$ from those where it is repulsive and $C < 0$. In the repulsive cases, we argued before that $\sigma_1 = \sigma_3$. The upper boundary is then the line $B = A + (N_c - 2)/\pi^2 T^2$. Below that line and above the line $B/A = N_c/2$, we again find square root dependence for both chiral and diquark fields. Attractive cases $(C > 0)$ require more care. Anticipating the following longer discussion of those regions of parameter space which are accessible, we remark that there are strict limits to the parameter ratio $C/B$ which can be realized. We choose $N_c = 3$ for the present discussion. A color octet interaction gives a ratio $C/B = f_\chi^O/f_8^O = -16/3$; a color singlet leads to $C/B = f_\chi^S/f_8^S = 2/3$. It is therefore clear from the definition of $B$ and $C$, Eq. (21), that any combination of octet and singlet interactions which produces a positive ratio $C/B$ must also satisfy $C/B \geq 2/3$.

The pattern of symmetry breaking now depends on the interaction. Let us start by the case $C/B = 2/3$, realized by a color singlet interaction. The minimum of $\Omega$ occurs for $\sigma_1 = 0$ and, since $\beta_2 = 0$ (Eq. (24)), $\sigma_3$ decouples from $\Delta$. The diquark field exhausts the strength alloted to the condensing colors, and chiral symmetry breaking acts independently on the third color. The upper boundary for this symmetry breaking pattern is the horizontal line $B = 3/(\pi^2 T^2)$. Let us now increase $C/B$ above $2/3$. The upper boundary moves down as illustrated in Fig. 1 and reaches the line $B = A + (N_c - 2)/(\pi^2 T^2)$ in the limit $C/B \rightarrow \infty$. For any intermediate value of $C/B \leq 2/3$, the chiral fields inside the wedge of mixed symmetry breaking satisfy $\sigma_3/\sigma_1 = 1 + (3 - 2A/B)/(C/B - 2/3)$. The sigma fields have again a square root dependence on the temperature.

It is remarkable that the overall structure of the phase diagram depends primarily on the critical ratio $B/A \sim N_c/2$. This follows because chiral condensation involves all $N_c$ colors, while quark Cooper pairs mix two colors only.

Now comes the question of understanding whether one can really access the richness of the phase diagram of Fig. 1 with a random matrix model. We noted above that there are strict limits on the parameter ratios which can actually be realized. As we shall demonstrate in the following section, the upper limit on the ratio $B/A$ is actually $N_c/2$. This precludes

the exploration of phases with $\Delta \neq 0$, and thus none of the random matrix model can support stable diquark condensates at zero chemical. It is possible to come close to a stable diquark phase in the case of an axial or a tensor interaction in the color singlet channel. In this limiting case, the diquark condensate can always be rotated into the chiral condensate for colors 1 and 2, while the remaining $N_c - 2$ colors break chiral symmetry independently. Even in this extreme case, the diquark condensate does not represent an independent thermodynamic phase.

## V. ALLOWED AND FORBIDDEN REGIONS OF PARAMETER SPACE

We now wish to demonstrate that the maximum attainable ratio $B/A$ is $N_c/2$. The quantity $B/A$ is a weighted ratio of the Fierz coefficients of the original interaction in chiral and diquark channels, Eq. (21). These coefficients were obtained from projecting certain chiral blocks, see Eqs. (10) and (12). Let us first consider a given Lorentz channel $C$, described by $n_C$ matrices $\Gamma_C$ ($n_C = 1, 1, 4, 4, 6$ when $C = S, P, V, A, T$, respectively). Its Fierz coefficient in the chiral channel is $f_\chi^a = (n_C/2)c^a$, where the color factor $c^a$ is $c^S = 1/N_c$ for a color singlet and $c^O = 2(N_c^2 - 1)/N_c^2$ for a color vector interaction, respectively. The Fierz coeffecient in the diquark channel is

$$f_\Delta^a = -2 \sum_{\mu=1,n_C} \frac{\text{Tr}[(C\gamma^5)\Gamma_C(C\gamma^5)\Gamma_C^T]}{\text{Tr}[(C\gamma^5)^2]^2} \frac{\text{Tr}[(i\lambda_2)\Lambda_a(i\lambda_2)\Lambda_a^T]}{\text{Tr}[\lambda_2^2]^2}, \tag{25}$$

where $\sum_{\mu=1,n_C}$ is a sum over the $n_C$ members of the Lorentz channel. The ratio of traces of Dirac matrices can be determined from their transposition property. Noting that

$$(C\gamma^5)\, \Gamma_C^T \,(C\gamma^5) = -\Gamma_C \quad \text{when } C = S, P, V, \tag{26}$$

$$(C\gamma^5)\, \Gamma_C^T \,(C\gamma^5) = +\Gamma_C \quad \text{when } C = A, T, \tag{27}$$

we deduce that ratio to be $-n_C/4$ when $C = S, P, V$ and $n_C/4$ when $C = A, T$. The ratio of traces of color matrices can be deduced from the completeness relations for the generators of $SU(N)$,

$$\sum_{a=1}^{N_c^2-1} \lambda_{\alpha\beta}^a \; \lambda_{\gamma\delta}^a = 2 \left( \delta_{\alpha\delta} \; \delta_{\beta\gamma} - \frac{1}{N_c} \delta_{\alpha\beta} \; \delta_{\gamma\delta} \right). \tag{28}$$

Thus, color contributes a factor $f_\Delta^{C|S} \sim -1/2$ for a singlet and $f_\Delta^{C|O} \sim 1 + 1/N_c$ for a vector interaction, respectively. For reference, we note that single-gluon exchange produces a ratio of Fierz coefficients $f_\Delta^O / f_\chi^O = 3/4$.

We now combine several Lorentz and color channels and try to obtain the largest ratio $B/A$. Large ratios are obviously realized by attractive quark-quark interactions. These channels have positive coefficients $f_\Delta^a$. They correspond to a Lorentz scalar, pseudoscalar, or vector with a color interaction in the $N_c^2-1$ channel or to a Lorentz tensor or pseudovector with a singlet color interaction. Their combination gives a ratio

$$\frac{B}{A} = \frac{\left( \Sigma_{S|O}^{-2} + \Sigma_{P|O}^{-2} + 4\Sigma_{V|O}^{-2} \right) (N_c + 1)/N_c + \left( 4\Sigma_{A|S}^{-2} + 6\Sigma_{T|S}^{-2} \right) 1/2}{\left( \Sigma_{S|O}^{-2} + \Sigma_{P|O}^{-2} + 4\Sigma_{V|O}^{-2} \right) 2(N_c^2 - 1)/N_c^2 + \left( 4\Sigma_{A|S}^{-2} + 6\Sigma_{T|S}^{-2} \right) 1/N_c} \tag{29}$$

It is now clear that $B/A$ is bounded from above as $B/A \leq N_c/2$, for $N_c > 2$. The upper bound can be reached by keeping only the last terms in numerator and denominator. This corresponds to either an axial or tensor interaction in a color singlet channel.

It is instructive to consider the phase diagram of a model with the limiting value $B/A = N_c/2$. We noted earlier that the coupling between chiral fields vanishes when the interaction is a color singlet: now, $C/B = 2/3$ which implies $\beta_2 = 0$, see Eq. (24). The phase diagram follows immediately. There is only one critical temperature $T_c = 2/(\pi^2 A)$ below which chiral and color symmetries are broken, and their fields satisfy $\sigma_3^2 = \Delta^2 + \sigma_1^2 = (2/A)(1 - T^2/T_c^2)$. The symmetry breaking pattern for color is thus $SU(N_c) \rightarrow SU(2) \times SU(N_c - 2)$. Colors 1 and 2 exhibit a diquark condensate, while chiral symmetry operates independently on the third color. However, one can rotate a given color broken solution $(\Delta, \sigma_1) = (\Delta_0, 0)$ into $(\Delta, \sigma_1) = (0, \Delta_0)$. This rotation brings the original state to one for which $\sigma_1 = \sigma_3$ and $\Delta = 0$. The initial state is thus equivalent to one of broken chiral symmetry, and the diquark condensate does not describe a thermodynamically independent phase. We show in the appendix that the chiral and diquark order parameters can be described by Banks-Casher formulas. However, because of the rotational symmetry, all three order parameters

are actually related to the same spectral correlator. Note also that we have $B = A$ when $N_c = 2$. The chiral and diquark fields can then always be related by a rotational symmetry. This follows from the pseudo-reality of $SU(2)$ QCD and has been considered in detail in Refs. [13] and [14].

We briefly return to the issue of implementing more flavor structure in the Dirac operator by including the flavor generators $\tau_i$. The additional flavor symmetry would contribute to the Fierz projections in the chiral and diquark channels. However, these additional factors would be those of an $SU(2)$ symmetry, and would therefore be equal in both channels. An additional flavor structure in the interaction cannot raise the ratio $B/A$ above $N_c/2$.

## VI. COMPARISON WITH A MICROSCOPIC MODEL

The phase diagram that we have obtained shares many features with those of the microscopic model of Berges and Rajagopal [2], and other NJL models [6]. We can summarize the three main ingredients of these models as follows. First, the four-fermion interaction respects the global chiral and color symmetries of QCD. Second, the coupling constants in the chiral and diquark channels are left as free parameters; particular choices of these parameters correspond to an interaction induced either by instantons or by single-gluon exchange. Third, the effects of asymptotic freedom are implemented by form factors whose actual form is model-dependent.

A comparison bewteen NJL-models and the present matrix models clearly shows what predictions on the phase diagram are protected by symmetry. To illustrate this, let us start from the effective potential given in Ref. [2], and take the limit of zero chemical potential. With a few obvious renaming of variables, we obtain

$$\Omega = A\Delta^2 + B\sigma^2 - 2 \int_0^\infty \frac{q^2 dq}{\pi^2} \Big\{ (N_c - 2) \Big\{ E_\sigma + 2T \log \Big( 1 + \exp[-E_\sigma/T] \Big) \Big\}$$
$$+ 2 \Big\{ E_\Delta + 2T \log \Big( 1 + \exp[-E_\Delta/T] \Big) \Big\} \Big\}, \tag{30}$$

where the single particle energies are $E_\sigma^2 \equiv q^2 + F^4\sigma^2$, $E_\Delta^2 \equiv q^2 + F^4(\sigma^2 + \Delta^2)$, and $F =$

18

$\Lambda_{\text{qcd}}^2/(q^2 + \Lambda_{\text{qcd}}^2)$ is an *adhoc* form factor. Following Berges and Rajagopal, we do not consider here that the chiral condensates can split in color space, and we thus retain a single chiral field, $\sigma_1 = \sigma_3 = \sigma$. Remarkably, the potential $\Omega$ gives a phase diagram identical to that of Fig. 1. We find again a single minimum to $\Omega$ for each set of parameters. This results in single phases separated by straight line boundaries of second order transitions. The general topology of the phase diagram is mostly set by color symmetry. The overall scale is however sensitive to form factors. Let us for instance choose the coupling constants such that $B/A < N_c/2$. For these ratios, our model has one critical line $B = N_c/(\pi^2 T^2)$ where chiral symmetry is restored. This line translates in the NJL model into the line $B = N_c \mathcal{F}(T)$, where

$$\mathcal{F}(T) \equiv 2 \int \frac{dq\, q}{\pi^2} F^4 \tanh[\frac{q}{2T}] \tag{31}$$

Thus the scale $1/(\pi^2 T^2)$ translates into $\mathcal{F}(T)$, which is sensitive to the particular choice of the form factor $F$. This of course implies that the actual value of the critical temperature is model-dependent. But the topology of the phase diagram, and in particular the line $B = N_c A/2$, is protected by symmetry.

Our approach can also be compared to the O(N) symmetric two-dimensional model of Chodos et al. [16]. This model is a generalization of the Gross-Neveu interaction to include pairing forces. Repeating the discussion of the previous section, one would infer a phase diagram similar to that of Fig. 1. Given the interaction of Ref. [16], the critical line $B = AN_c/2$ becomes $A - B = 0$. In Ref. [16], $A - B$ actually corresponds to a parameter $\delta$ which determines which of the chiral $(A - B > 0)$ or the diquark $(A - B < 0)$ condensates exists in the vacuum. The parameter $\delta$ is further shown to be invariant under renormalization. This result is consistent with the fact that the topology of the phase diagram only depends on global symmetries.

Although the present discussion indicates that the random matrix and NJL-type microscopic approaches share fundamental features, they differ in one essential point. NJL-studies generally assume from the start a potential of the form of Eq. (23) on the basis of symmetry

considerations. The coupling contants $A$, $B$, and $C$, may be related to one another in specifically motivated cases, but are in general taken as free parameters whose range of variation is dictated by the phenomenology to be reproduced. By contrast, random matrix models start out at a more microscopic level. We first selected certain types of interactions satisfying global symmetries, and then mimicked the dynamics by means of a random background. We also confined ourselves to Hermitean matrix models, in which a meaningful relation between order parameters and spectral properties can be found. As a result of working at a microscopic level, the coupling parameters of the potential in Eq. (23) satisfy strong constraints such as $B/A \leq N_c/2$. These constraints are not deduced from phenomenology but are now inherited from the dynamics of the primary interactions which have been integrated over. Starting from a more microscopic level thus has the clear advantage of implementing those dynamical constraints, while still permitting the construction of the desired global symmetries.

When comparing with microscopic models, it is also necessary to consider exchange effects. Random matrix models include only direct terms. Exchange terms involve quark fields with unequal matrix indices $k$ and $l$ in Eqs. (9) and (16), and are therefore $1/N$ suppressed. To take exchange effects explicitly into account, we must modify by hand the four-fermion interaction produced by integration over the random background. This amounts to adding to the original four-fermion interaction its Fierzed transformed expression [15]. One way of proceeding is to fine tune the variances of the random background in order to reproduce the modified four-fermion interaction. It turns out that only scalar interactions produce exchange effects that alter the chiral channel; exchange actually changes the sign of the Fierz coefficient in that channel. The modified interaction is repulsive for chiral condensation and may thus favor diquark condensation. This opens the possibility of exploring the region of the phase diagram above the line $B/A > N_c/2$. However, the matrix model that would mimic exchange is non-Hermitean, a case which is ouside the scope of this paper.

A final comment concerns the similarities between single-gluon exchange and instanton-induced interactions in regard with the explored region of the phase diagram. To mimic

single-gluon exchange we choose a vector interaction, which produces $B/A = 3/4$. To understand how to mimic an instanton-induced interaction, we first notice that it conserves chirality (we assume here an interaction arising by scattering on single instantons). Thus, a genuine matrix model would combine scalar, pseudoscalar, and tensor interactions, and would then be very different in character from single-gluon exchange. It turns out that an instanton-induced interaction actually produces the same ratio $B/A = 3/4$ as single gluon exchange, provided exchange effects are taken into account [8]. This result is not surprising. The instanton-induced interaction is generated by integration over a classical gluon background which couples to quarks as a color vector. A correct and consistent treatment must respect the vector nature of the interaction and should produce a ratio $B/A = 3/4$. Therefore, QCD and any of its consistent approximations should lie on the line $B/A = 3/4$.

## VII. CONCLUSIONS

In this paper, we have introduced a random matrix model that can in principle admit both chiral and diquark condensations and have studied the competition of these two forms of order at zero chemical potential. We have considered interactions that are Lorentz invariant in the vacuum and gauge symmetric and have displayed the rich structure of the ensuing phase diagram in parameter space. The topology of the phase diagram is mostly governed by color symmetry. Its exploration requires the variation of only two ratios of Fierz coupling constants. We have further argued that there exist strong constraints on the values that these ratios can actually achieve. For interactions represented by Hermitean matrices, the ratio of the coupling constant in the chiral channel to that in the diquark channel is necessarily less than the critical value $N_c/2$ required to favor the formation of Cooper pairs. Thus, none of the present random matrix models can support stable diquark condensates.

Our arguments are primarily based on symmetry considerations that also apply to QCD. This leads us to the conclusion that no mean-field treatment of QCD with two light flavors

can support independent diquark condensates at zero chemical potential. This conclusion does of course respect the phenomenological evidence that the QCD vacuum spontaneously breaks chiral symmetry, but not color symmetry. The main message of our approach, however, is to emphasize that the coupling constants of an effective potential are constrained by the underlying symmetries of the interaction they mean to represent. Determining these constraints in a given physical situation helps rule out certain forms of order on the basis of symmetry alone.

## NOTE ADDED IN PROOF

After the completion of this work, we have learned about a related study of the phase structure of QCD in the vacuum, summarized in S. Ying, Phys. Lett. B **285**, 341 (1992); Ann. Phys. (NY) **250**, 69 (1996). We thank S. Ying for pointing these references to us.

## APPENDIX

In this appendix, we explore further the case of an axial interaction with a color singlet structure. As we showed in Section V, this interaction achieves a ratio $B/A = 3/2$. We found before that the gap equations yielded solutions with a finite diquark condensate which are degenerate with those of pure broken chiral symmetry. We now wish to derive Banks-Casher relations for the condensates. We show that the degeneracy of the solutions forces all condensates to be related to the same component of the Dirac spectrum.

The two chiral and the diquark condensates can be obtained from the partition function by taking

$$\langle \psi_{1\alpha}^{\dagger} \psi_{1\alpha} \rangle = \lim_{m_1 \to 0} \lim_{N \to \infty} \frac{1}{2NN_f} \left. \frac{\partial \log Z(T)}{\partial m_1} \right|_{\eta=0, m_3=0} \quad \text{when } \alpha = 1, 2, \tag{32}$$

$$\langle \psi_{1\alpha}^{\dagger} \psi_{1\alpha} \rangle = \lim_{m_3 \to 0} \lim_{N \to \infty} \frac{1}{NN_f} \left. \frac{\partial \log Z(T)}{\partial m_3} \right|_{\eta=0, m_1=0} \quad \text{when } \alpha = 3, \tag{33}$$

$$\langle \psi_2^T P_\Delta \psi_1 \rangle = i \lim_{\eta \to 0} \lim_{N \to \infty} \frac{1}{N} \left. \frac{\partial \log Z(T)}{\partial \eta^*} \right|_{m_1=0, m_3=0}. \tag{34}$$

22

Here, as usual, it is important to take the thermodynamic limit $N \to \infty$ first to obtain physically meaningful quantities for the condensates [12]. The derivatives can be evaluated in a formal way. Integrating the partition function in Eq. (1) over the random background, an operation which we represent here by brackets, we obtain

$$Z(T) = \langle \exp \mathrm{Tr} \log i\mathcal{D} \rangle \tag{35}$$

where $\mathcal{D}$ is the flavor block matrix

$$\mathcal{D} = \begin{pmatrix} \mathcal{H} + \mathcal{T} + im & \eta P_\Delta \\ -\eta^* P_\Delta^\dagger & -\mathcal{H}^T + \mathcal{T} - im \end{pmatrix}. \tag{36}$$

Taking the derivatives in Eqs. (32), (33), and (34), we have

$$\langle \psi_{1\alpha}^\dagger \psi_{1\alpha} \rangle = \lim_{m_1 \to 0} \lim_{N \to \infty} \frac{i}{NN_f} \left\langle \frac{\det i\mathcal{D}}{\langle \det i\mathcal{D} \rangle} \mathrm{Tr} \left[ P_1 \left( \mathcal{D}_{11}^{-1} - \mathcal{D}_{22}^{-1} \right) \right] \right\rangle \bigg|_{\eta=0, m_3=0} \quad (\alpha = 1, 2), \tag{37}$$

$$\langle \psi_{1\alpha}^\dagger \psi_{1\alpha} \rangle = \lim_{m_3 \to 0} \lim_{N \to \infty} \frac{i}{NN_f} \left\langle \frac{\det i\mathcal{D}}{\langle \det i\mathcal{D} \rangle} \mathrm{Tr} \left[ P_3 \left( \mathcal{D}_{11}^{-1} - \mathcal{D}_{22}^{-1} \right) \right] \right\rangle \bigg|_{\eta=0, m_1=0} \quad (\alpha = 3), \tag{38}$$

$$\langle \psi_2^T P_\Delta \psi_1 \rangle = \lim_{\eta \to 0} \lim_{N \to \infty} \frac{-i}{N} \left\langle \frac{\det i\mathcal{D}}{\langle \det i\mathcal{D} \rangle} \mathrm{Tr} \left[ P_\Delta \mathcal{D}_{12}^{-1} \right] \right\rangle \bigg|_{m_1=0, m_3=0}, \tag{39}$$

where the color operators $P_1 = \mathrm{diag}(1, 0, 0)$ and $P_3 = \mathrm{diag}(0, 0, 1)$ project onto colors 1 and 3 respectively. To evaluate the matrices $\mathcal{D}_{11}^{-1}$, $\mathcal{D}_{22}^{-1}$, and $\mathcal{D}_{12}^{-1}$, one makes use of the fact that $\mathcal{H}$ is color diagonal, $\mathcal{H} = \mathrm{diag}(H, H, H)$, and that $H$ satisfies $C\gamma^5 H^T C\gamma^5 = H$. A diagonalization of the flavor block matrices gives then

$$\langle \psi_{1\alpha}^\dagger \psi_{1\alpha} \rangle = \lim_{m_1 \to 0} \lim_{N \to \infty} \frac{1}{N} \left\langle \frac{\det i\mathcal{D}}{\langle \det i\mathcal{D} \rangle} \frac{m_1}{(H + \mathcal{T})^2 + m_1^2} \right\rangle \quad (\alpha = 1, 2), \tag{40}$$

$$\langle \psi_{1\alpha}^\dagger \psi_{1\alpha} \rangle = \lim_{m_3 \to 0} \lim_{N \to \infty} \frac{1}{N} \left\langle \frac{\det i\mathcal{D}}{\langle \det i\mathcal{D} \rangle} \frac{m_3}{(H + \mathcal{T})^2 + m_3^2} \right\rangle \quad (\alpha = 3), \tag{41}$$

$$\langle \psi_2^T P_\Delta \psi_1 \rangle = i \lim_{\eta \to 0} \lim_{N \to \infty} \frac{1}{N} \left\langle \frac{\det i\mathcal{D}}{\langle \det i\mathcal{D} \rangle} \frac{\eta}{(H + \mathcal{T})^2 + |\eta|^2} \right\rangle, \tag{42}$$

We thus see that the three order parameters are related to the same spectral properties of the Dirac operator. This result confirms the degeneracies of the solutions with finite diquark fields with those of broken chiral symmetry.

## ACKNOWLEDGEMENTS

# REFERENCES

[1] For recent discussions of the QCD phase diagram, see K. Rajagopal, hep-ph/9908360; M. A. Halasz, A. D. Jackson, R. E. Shrock, and M. A. Stephanov, J. J. M. Verbaarschot, Phys. Rev. **D58** (1998) 096007, and references therein.

[2] J. Berges and K. Rajagopal, Nucl. Phys. **B538** (1999) 215.

[3] For recent reviews, see A. Ukawa, Nucl. Phys. **A638** (1998) 339; E. Laermann, Nucl. Phys. **B63** [Proc. Supp.] (1998) 114.

[4] B. Barrois, Nucl. Phys. **B129** (1977) 390. D. Bailin and A. Love, Phys. Rept. **107** (1984) 325.

[5] M. Alford, K. Rajagopal, and F. Wilczek, Phys. Lett. **B422** (1998) 247.

[6] T. M. Schwarz, S. P. Klevansky, and G. Papp, nucl-th/9903048.

[7] G. W. Carter and D. Diakonov, Phys. Rev. **D60** (1999) 016004.

[8] R. Rapp, T. Schäfer, E. V. Shuryak, and M. Velkovsky, Phys. Rev. Lett. **81** (1998) 53; hep-ph/9904353.

[9] E. V. Shuryak and J. J. M. Verbaarschot, Nucl. Phys. **A560** (1993) 306; J. J. M. Verbaarschot, Phys. Rev. Lett. **72** (1994) 2531; Phys. Lett. **B329** (1994) 351; For a review, see J. J. M. Verbaarschot, hep-ph/9902394.

[10] T. Banks and A. Casher, Nucl. Phys. **B169** (1980) 103.

[11] E. Brézin and A. Zee, Nucl. Phys. **B402** (1993) 613; A. D. Jackson, M. K. Sener, and J. J. M. Verbaarschot, Nucl. Phys. **B479** (1996) 707; G. Akemann, P. H. Damgaard, U. Magnea, and S. Nishigaki, Nucl. Phys. **B487** [FS] (1997) 721; E. Kanzieper and V. Freilikher, Philosophical Magazine **B77** (1998) 1161; M.K. Sener, J.J.M. Verbaarschot, Phys. Rev. Lett. **81** (1998) 248; K. Splittorff, Nucl. Phys. **B548** (1999) 613.

[12] A. D. Jackson and J. J. M. Verbaarschot, Phys. Rev. **D53** (1996) 7223.

[13] D. Diakonov and V. Petrov, in *Quark Cluster Dynamics*, Lecture Notes in Physics, edited by K. Goeke, P. Kroll, and H. Petry (Springer-Verlag, Berlin,1992) p. 288; A. Smilga and J. J. M. Verbaarschot, Phys. Rev. **D51** (1995) 829. J. B. Kogut, M. A. Stephanov, and D. Toublan, Phys. Lett. B **464**, 183 (1999).

[14] D. Diakonov, H. Forkel, and M. Lutz, Phys. Lett. **B373** (1996) 147.

[15] See for example S.P. Klevansky, Rev. Mod. Phys. **64**, 649 (1992).

[16] A. Chodos, F. Cooper, W. Mao, H. Minakata, and A. Singh, hep-ph/9909296.

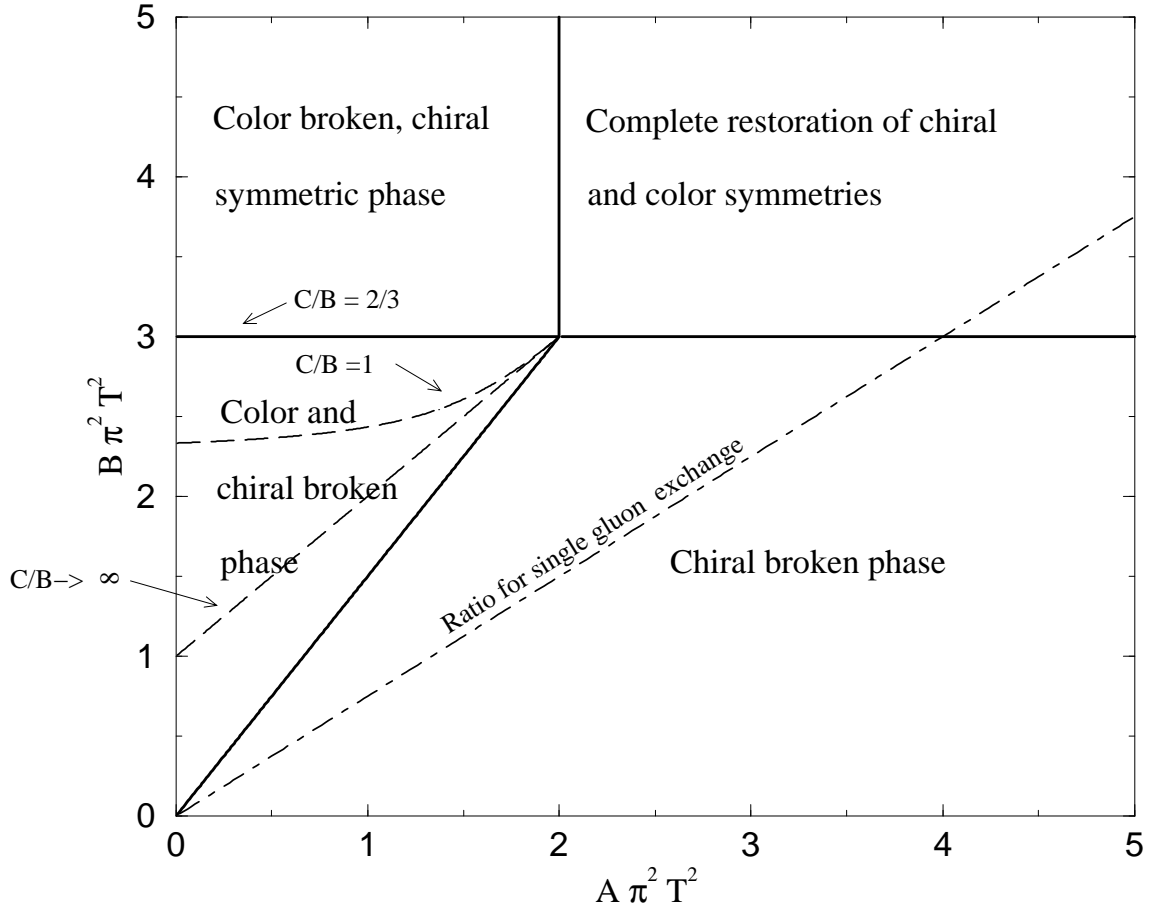[17] D. Weingarten, Phys. Rev. Lett. **51** (1983) 1830.

FIG. 1. The phase diagram in parameter space for $N_c = 3$. The horizontal axis represents the coupling constant in the diquark channel, the vertical axis represents that in the chiral channel. The solid curves are second-order phase transitions. The long-dashed lines correspond to the upper boundary of the phase where both color and chiral symmetries are broken. We show this boundary for various values of the ratio of coupling constants in the chiral and the chiral-$\lambda_8$ channels (see text). The dot-dashed line is the line of constant ratio $B/A = 3/4$ obtained with single gluon exchange and $N_c = 3$. This line does not cross any phase with a finite diquark condensate.